Cellulose (2009) 16:975–982
DOI 10.1007/s10570-009-9331-z

Cellulose structural arrangement in relation to spectral changes in tensile loading FTIR

Lennart Salmén · Elina Bergström

Received: 11 February 2009 / Accepted: 29 May 2009 / Published online: 13 June 2009

Abstract In order to utilise wood and wood fibres in advanced materials, a better understanding of the mechanical material characteristics and the interactions among the components is necessary. For this purpose, FTIR was explored together with mechanical loading as a means of studying the molecular responses to the loading of spruce wood and cellulose paper material. A linear shift of absorption bands was detected as the loading was applied. In relation to the applied stress these shifts were higher under moist conditions than under dry ones but they were similar with regard to the strains applied. There were no shifts detected in bands related to lignin or the hemicelluloses. The results are interpreted as reflecting a parallel arrangement of the load bearing component, the cellulose ordered structure, and the moisture accessible regions in the cellulose microfibril structure. This therefore represents an equal strain loaded system.

Keywords Cellulose · Deformation · Fourier transform infrared (FTIR) · Moisture · Structure · Wood

L. Salmén (✉) · E. Bergström
INNVENTIA (former STFI-Packforsk), Box 5604, 114 86 Stockholm, Sweden
e-mail: Lennart.salmen@innventia.com

Introduction

Wood is an extremely stiff and strong material in relation to its density. To a large extent this fact is related to the properties of the cellulose component which, with its crystalline microfibrils mainly oriented in the longitudinal direction of the fibres, provide for the strength and stiffness of the wood. The angular dependence of strength properties in relation to the cellulose microfibrillar angle is clearly demonstrated (Cave 1968; Page and El-Hosseiny 1983). However, when it comes to more complicated loading modes than to pure longitudinal tension/compression, e.g. transverse properties or shearing, the involvement of the other major components in the wood fibre cell wall, i.e. the hemicelluloses and the lignin, are more apparent (Bergander and Salmén 2002; Salmén 2004), while knowledge about the mechanisms is very limited. In order to overcome this lack of knowledge, more detailed descriptions of the ultrastucture of the fibre wall and of the interactions among the components, in a mechanical sense, are required.

Using spectroscopic techniques, it is possible to study the response to stresses on the molecular level and analyse the mechanical interactions among components on the in situ construction of cellulose fibres and wood materials. In this instance, both Fourier Transform Infrared (FTIR) and Raman spectroscopy were utilised (Åkerholm and Salmén 2001; Eichhorn et al. 2001; Gierlinger et al. 2006; Hinterstoisser et al.

2001; Sturcová et al. 2006). In particular Raman spectroscopy has been used extensively to unravel the structure and arrangement of the wood polymers in the cell wall as well as its dependence on the loading of the material, as demonstrated by Gierlinger et al. (2006). Thus, it has been well demonstrated that the loading applied to a wood fibre results in a substantial band shift of the main Raman absorption peak of the cellulose, arising at 1,097 cm^{-1} and related to the C–C and C–O stretching along the cellulose chain. The shift of this peak was directly related to the load. However, no shift was detected in these Raman studies for the main lignin peak of 1,608 cm^{-1} (Gierlinger et al. 2006), indicating absence of load contribution. Utilising dynamic FTIR, where the time-resolved response to dynamic loading is interpreted at the molecular level, a close cooperation has been shown between glucomannan and cellulose for wood fibres (Åkerholm and Salmén 2001). In addition, it has not been possible to verify the involvement of lignin in the stress transfer from such measurements (Åkerholm and Salmén 2003). One advantage of using FTIR is that it is more easily adapted to studies under moist conditions (Åkerholm and Salmén 2004). This is an important factor, considering the high hygroscopy of the wood polymers and its influence on the mechanical properties of the wood material. By utilising deuterated water for producing the moist air, instead of normal water, it is also possible to separate the absorption bands of the moisture attached to accessible regions from those hydrogen bonding regions that are not affected by moisture (Hofstetter et al. 2006).

Studies utilising the effects of loading on the band shifts of normal FTIR suffer from the ability to resolve the rather broad absorption peaks generally associated with IR. Elaborate computational procedures have often been required to resolve the spectra satisfactorily (Sturcová et al. 2006). However, by carefully stabilising the measuring parameters and running the FTIR at the highest resolution possible, the possibility exists for resolving the band shift even for such a complicated material like the wood structure. In this paper, this possibility is explored with regard to the deformation behaviour of spruce wood, comparing the differences between dry and moist conditions. The focus has been on the main structural elements in cellulose responsible for load transfer, i.e. that of the glucose ring and the C–O-C deformation, showing a FTIR absorption peak at 1,160 cm^{-1} (Liang and Marchessault 1959b; Tsuboi 1957; Tashiro and Kobayashi 1991), and of the 3OH···O5 intramolecular hydrogen bond absorbing at 3,348 cm^{-1} (Fengel 1993; Hinterstoisser et al. 2003; Ivanova et al. 1989; Liang and Marchessault 1959a) as illustrated in Fig. 1. The intention with this analysis has been to utilize the in situ FTIR-method to distinguish between potential distributions of crystalline and disordered, moisture accessible, parts within the cellulose microfibrils.

Experimental

Materials

The wood material studied was taken at breast height from the mature wood (annual rings 30–35) of a spruce log, *Picea abies L Karst.,* grown on fertile soil in the middle of Sweden. A section was cut from the outer part of a fresh log and stored at +4 °C until a sample was prepared. Wood specimens of pieces from the earlywood were prepared using microtome cutting under wet condition. They were cut, in the tangential plane, with a thickness of 40 μm, a length of 25 mm and a width of 20 mm, with the fibre axis in the direction of the length. The wood cuttings were mounted in their wet condition in a stretching device (length direction in the direction of loading) and allowed to condition for 60 min at 30 °C, 90% RH, while maintaining the load at zero force.

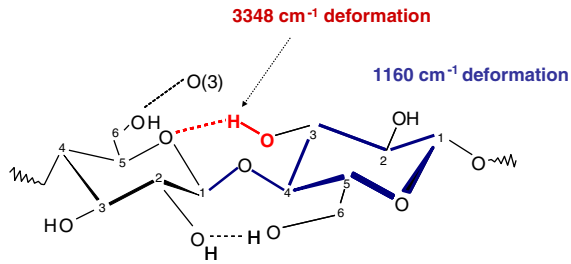

Fig. 1 Structure of a cellulose molecule, with the main contributing stress transferring structures illustrated, viz. that of the C–O–C glycoside bond and the glucose ring, responsible for the vibration peak at 1,160 cm^{-1}, as well as that of the 3OH···O5 intramolecular hydrogen bond, responsible for the vibration peak at 3,348 cm^{-1}

Cellulose samples were prepared from a spruce dissolving pulp with a cellulose content of 98%. This was provided by Borregaard. The pulp was homogenized by pumping it at a consistency of 0.5% three times through a slit (0.3–0.4 mm) in a laboratory homogenizer (Gaulin Corp., Everett, MA, USA). This resulted in a large degree of fibrillation of the fibres as well as fibre splitting. Oriented sheets with a grammage of 20 g/m^2 and a thickness of about 40 μm were made on a Formette Dynamique at a rotation speed of 1,600 rpm. The samples used in the experiments were cut into dimensions of $\sim 25 \times 20$ mm, with the direction of the fibres parallel to the longitudinal direction.

FTIR measurements

FTIR spectra were recorded on an FTS 6000 spectrometer (Digilab Inc., Randolph, MA, USA) in transmission mode. A DTGS (deuterated triglycine sulphate) detector was used and the IR radiation was polarized by a KRS5 wire grid polarizer at 0° in relation to the stretching direction. An optical filter was added after the polarizer to reduce the spectral range (3,950–700) cm^{-1}.

The samples were mounted between two parallel jaws in a specially constructed tensile stretcher, a Polymer Modulator (PM-100), with the main fibre direction in the direction of the load, see Fig. 2. The PM-100 was placed into a Temperature Control System (TC-100) (MAT-Manning Applied Technology Inc., Troy, ID, USA) and mounted in the sample compartment.

Spectra were recorded at 1 cm^{-1} spectral resolution (data acquired each 0.5 cm^{-1}), using an average of 8 scans at each strain level. Spectra were baseline corrected at 2,000 cm^{-1} and the 1st derivative was used for determining the peak position for each specific absorption peak investigated.

Prior to making the FTIR measurements the mounted sample was conditioned in the testing climate for 60 min. During this time the sample was kept in a straight position using a pre-load of ca 0.5 N. Spectra were recorded at successively increasing loads every other minute, from 0.5 N up to the rupture of the sample which occurred between the grips. In order to obtain a stable stress situation during the recording of the FTIR spectra the load was allowed to relax for 1 min. (15% change in load) at each applied loading before the measurement started. The load was taken as the average load registered at the start and the end of the respective FTIR measurements. The strain was based on the original clamping length of the sample, i.e. ~20 mm, while the stress was based on the macroscopic dimensions of the sample.

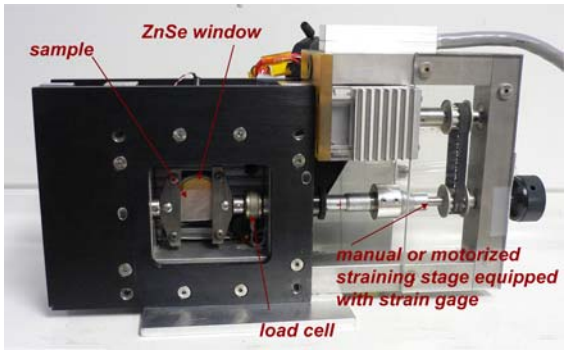

Fig. 2 Polymer Modulater (PM-100). The sample is placed between the two clamping jaws having a distance of ca 20 mm. The straining compartment is encapsulated allowing for moist air to be introduced at a controlled temperature into the measuring chamber (cover plate with ZnSe window for IR-radiation to be mounted on the side of the compartment). The straining of the sample is done with the manual gage to the right of the figure. The stress and strain imposed were registered digitally

Humidity control

In order to control the environmental conditions, the temperature in the sample chamber was controlled at 30 °C throughout all the experiments. The relative humidity in the chamber was controlled by a continuous stream of air, either totally dry or with a relative humidity, RH, of 90% based on deuterium oxide vapour. An RH of 90% was achieved by saturating air at a lower temperature than that of the measurement, by passing the air flow through a flask of deuterium oxide placed in a thermostat bath. Technically, pure deuterium oxide (99 atom-%) provided by Sigma-Aldrich Inc, Milwaukee, WI, USA was used in the latter case.

Results

Figure 3 shows the stress–strain graph for the spruce wood samples under the two different climatic conditions of 0% and 90% RH. Under both

conditions, an almost linear elastic behaviour was registered until the rupture of the wood sample, very similar to tests of single spruce wood fibres (Burgert et al. 2008; Gierlinger et al. 2006;). Naturally the moist sample displayed a lower stiffness due to the softening effect exerted by the moisture (Kersavage 1973).

Examining the spectral changes as affected by the stress applied to the wood sample, it was clear that a substantial shift in the position of the peak maximum occurred for several absorption bands. This is exemplified in Fig. 4, showing the shift obtained for the absorption peak at 1,160 cm^{-1}, C–O–C vibration,

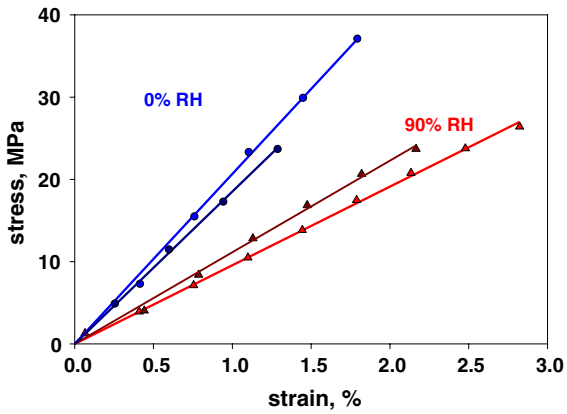

Fig. 3 Stress–strain properties of earlywood of spruce wood tested in the longitudinal direction under two different climates 0 and 90% RH, respectively. The variability between the samples is within the normal range of variation seen for well matched wood samples

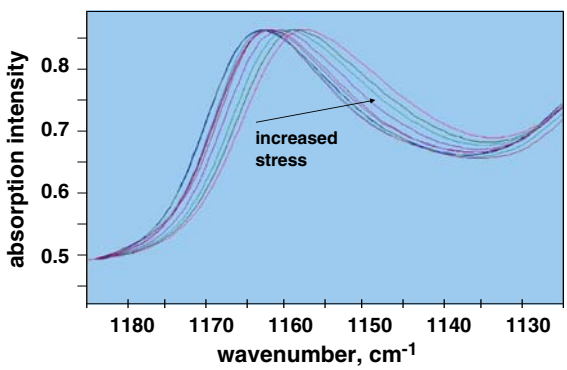

Fig. 4 Absorption spectra of the C–O–C vibration peak at 1,160 cm^{-1} for a spruce wood sample under dry conditions subjected to increasing stress levels. With the increase in stress, the peak shifted towards lower wavenumbers

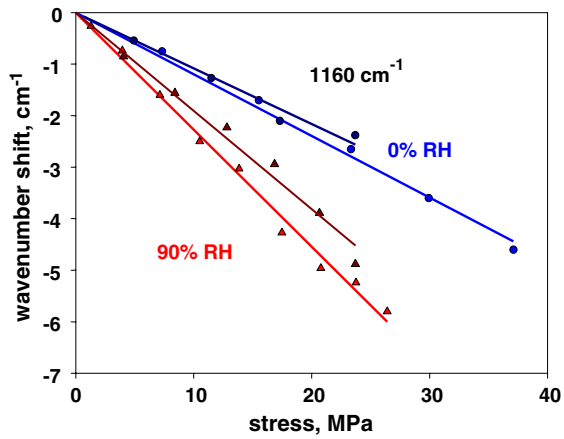

Fig. 5 Shift of the absorption peak at 1,160 cm^{-1}, as a function of the applied stress for a spruce wood sample tested in the longitudinal direction, under dry and moist 90% RH conditions, respectively

when successively loaded from 0 up to 24 MPa at 0% RH. In total the shift was almost 6 wavenumbers, decreasing as the stress was applied. This decrease in wavenumber signifies an increase in the length of the covalent bonds involved in the vibration absorption, i.e. a decrease in the force constant of the bond (Wool 1981).

Figure 5 shows the shift for the absorption peak at 1,160 cm^{-1}, plotted against the applied stress for the spruce wood sample at 0 and 90% RH, respectively. It is obvious that the shift was linear with the applied stress being in agreement with previous Raman studies on the effect of stress on this particular vibration for wood samples related to the C–O–C stretching (Eichhorn et al. 2001; Gierlinger et al. 2006). Under the moist condition, i.e. 90% RH, the shift decreased faster with the applied stress. Other vibrations related to the cellulose chain, such as the COH bending at 1,424 cm^{-1} (Hinterstoisser et al. 2001) and the C–O vibration at 1,060 cm^{-1} (Tsuboi 1957; Fengel 1991) also showed a similar linearly decreasing peak position with the stress applied.

For the hydrogen bonding region of 3,000–3,500 cm^{-1}, a main shift was detected for the 3OH···O5 intramolecular hydrogen vibration at 3,348 cm^{-1} (Fengel 1993; Ivanova et al. 1989; Liang and Marchessault 1959a) as shown in Fig. 6. Here, the shift in wavenumber was found to increase, in a linear manner with the stress applied, which was a direction of the shift previously suggested for this

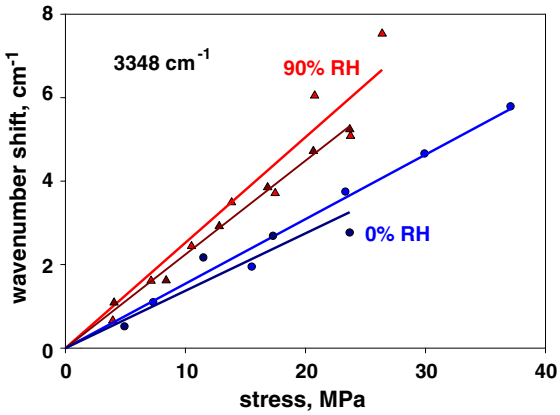

Fig. 6 Shift of the absorption peak at 3,348 cm^{-1}, as a function of the stress applied, for a spruce wood sample tested in the longitudinal direction under dry and moist 90% RH conditions, respectively

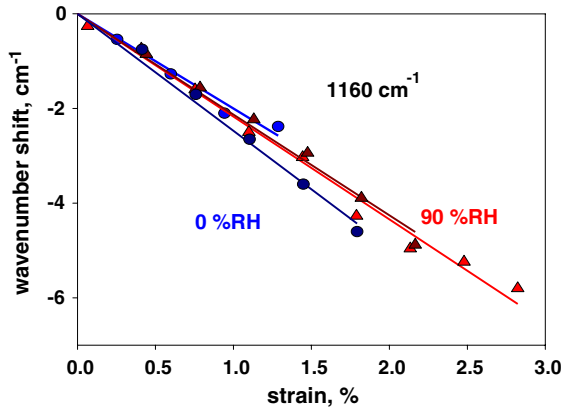

Fig. 7 Shift of the absorption peak at 1,160 cm^{-1}, as a function of the applied strain for a spruce wood sample tested in the longitudinal direction under dry and moist 90% RH conditions, respectively

absorption peak (Gierlinger et al. 2006). This should be related to a reduction in the OH bond length, due to a weakening of the hydrogen bonding under straining. A strong influence of the hydrogen bonding on this absorption peak has been demonstrated (Marechal and Chanzy 2000). For the moist condition, the shift in wavenumber was greater per unit stress than at zero humidity, which is similar to the larger shift under moist conditions that was also seen for the 1,160 cm^{-1} absorption peak.

If the peak shifts were plotted as a function of strain instead of stress, it was obvious that the shifts were very similar for the two climatic conditions of 0 and 90% RH, as seen in Figure 7 for the 1,160 cm^{-1} absorption peak. This indicates that the load distribution in the tensile testing of wood could be related to that of an equal strain situation, i.e. in both climates, the cellulose load bearing component is strained to the same extent on the molecular level, when strained to the same extent on the macroscopic level.

On examining vibrations that are not related to cellulose in the FTIR spectra, it was clear that such vibrations did not show any shift with the applied stress, as exemplified in Fig. 8 for the lignin aromatic ring vibration at 1,509 cm^{-1} (Colthup et al. 1990). In fact, there was no vibration found that was specifically related to either lignin (1,509, 1,591 cm^{-1}), xylan (1,735, 1,460 cm^{-1}) or glucomannan (870, 810 cm^{-1}) vibrations to show a shift in peak position with the applied stress, neither at 0 or 90% RH. This

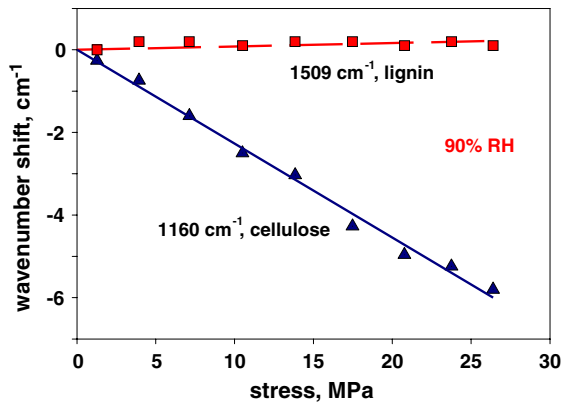

Fig. 8 Shift of the absorption peak at 1,160 cm^{-1}, related to cellulose, and the absorption peak at 1,509 cm^{-1}, related to lignin, as a function of the applied strain for a spruce wood sample tested in the longitudinal direction under moist 90% RH conditions

behaviour was similar to that found by Gierlinger et al. (2006) for the main lignin Raman signal at 1,602 cm^{-1} attributed to the aryl stretching band (Agarwal 1999), which, under deformation, was found virtually unaffected, while a strong shift was noted for the cellulose absorption peaks (Gierlinger et al. 2006).

Tests were also carried out on a pure cellulose material, thus excluding contributions to the absorptions from other carbohydrate components. Figure 9 shows the stress–strain properties of this paper material of oriented cellulose tested at 0 and 90% RH. As this material is less anisotropic, when

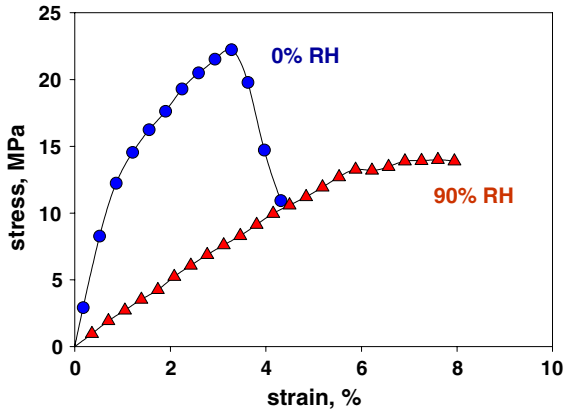

Fig. 9 Stress–strain properties of oriented cellulose sheets tested in the fibre direction under two different climates, 0 and 90% RH, respectively. Under the dry condition, 0% RH, the sample exhibits post failure behaviour, i.e. it is possible to follow the decreasing load after the failure stress

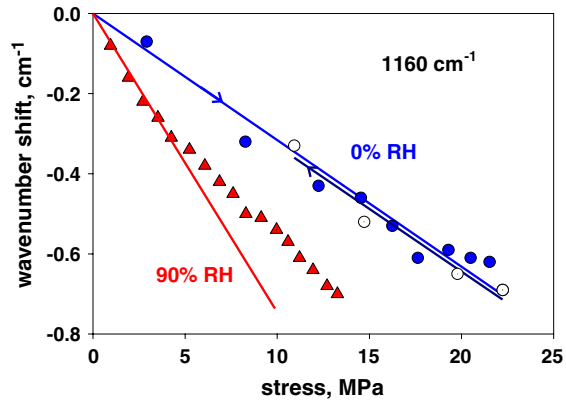

Fig. 10 Shift of the absorption peak at 1,160 cm^{-1}, as a function of the stress applied for oriented cellulose sheets tested in the fibre direction under dry and moist 90% RH conditions, respectively. *Unfilled symbols* represents decreasing load

compared to wood (fibres and cellulose fibrils less oriented in the loading direction), and the fact that the material has rather few bonding points per fibre, due to its low basis weight, this material showed a more ductile behaviour, as compared to the wood material shown in Fig. 3. Thus, under dry conditions the sample did not break abruptly but a post failure behaviour was seen.

As seen in Fig. 10, the shifts in the peak position for the cellulose vibration at 1,160 cm^{-1} were smaller than those seen for the wood sample. By utilising data from the entire peak spanning 1,170–1,156 cm^{-1} in wavenumber a resolution of 0.05 cm^{-1} for the peak position was achieved. It should here also be recognized that the load causes a slight increase in the orientation of the cellulose chain in the direction of the loading. This also resulted in an increase in the absorption peak height in the polarized spectra. For the cellulose, it was also clear that, under the moist condition, i.e. 90% RH, the shift was larger as a function of the applied stress. Under the dry condition, the peak shift was linear as a function of the stress applied, also after the sample had reached its maximum load and the stress was decreasing, unfilled symbols in Fig. 10. Under the moist condition of 90% RH, linearity was only observed for the initial phase of the loading.

Discussion

It is clear from these measurements that mechanical loading results in peak shifts in the cellulose vibrations, which may be detected with FTIR. For a material with highly oriented cellulose molecules, as in softwood fibres with a low fibrillar angle, a substantial shift, linear with the applied stress, was observed. It is therefore quite clear that straining this structure in the direction along the molecules will result in an elongation of the C–O–C bond as well as of the glucose ring. The particular vibration assigned to these structures, i.e. the one at 1,160 cm^{-1}, may be characteristic for all of the C–O–C bonds of the wood carbohydrate polymers although it is most strongly associated to the cellulose (Åkerholm and Salmén 2001). In addition the 3OH···O5 intramolecular hydrogen bond in cellulose will be strained but this will result in a weakening of the hydrogen bond itself, which is the reason why the 3OH vibration will become stronger with the loading of the sample. Hence the measurements made here strengthen the conclusion made of the importance of these structures for stress distribution in cellulose.

The fact that the shift of the vibration peaks under the two different climates (0 and 90% RH) are similar as a function of the strain, but different as a function of the stress, indicates that the deformation involved is more that of an equal strain situation than that of an equal stress one. It is well recognized that, in the longitudinal direction of wood fibres, it is the cellulose that is the main load bearing structure of the wood. As

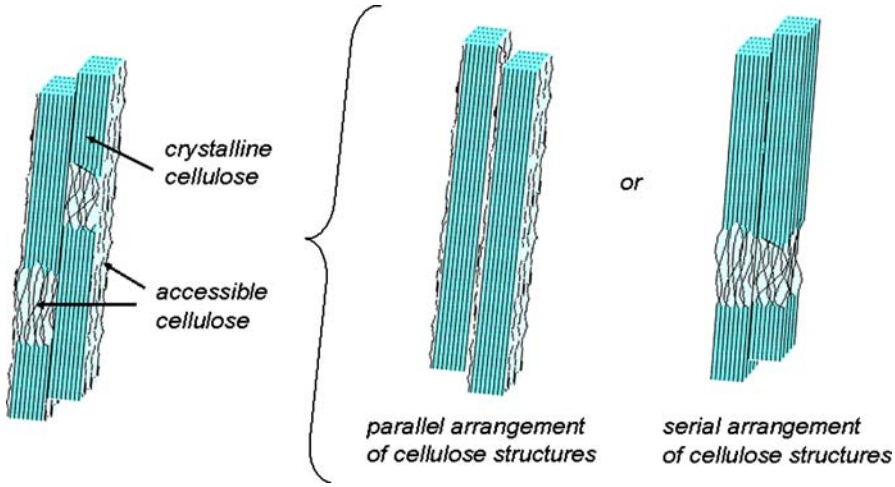

Fig. 11 Illustration of the cellulose microfibril structure with distribution of crystalline and moisture accessible cellulose regions. For the discussion the structure is schematically illustrated as two extreme cases, viz. that of accessible regions along the sides of the microfibrils, a *parallel* arrangement of the components or that of accessible regions along the length of the microfibrils, a *serial* arrangement of the components

seen by the analysis here this load bearing on the molecular level is greatly affected by the moisture content. Considering the structure of the cellulose, the distribution of moisture-absorbing structures in the cellulose microfibrils (Salmén 1990) must be taken into consideration. The existence of disturbed zones along the length of the microfibrils (Rowland and Roberts 1972) together with the contribution from the surfaces along the sides of the fibrils (Wickholm et al. 1998), need to be recognised, as illustrated in Fig. 11. When looking at the stress distribution over the accessible and non-accessible regions, the structure could be simplified into two basic structures, with only disturbed zones representing a case of equal stress, when the load is applied along the microfibrils, or with only moisture accessible surface areas that represent a case of equal strain in the longitudinal loading of the microfibrils, Fig. 11. For the case of the wood structure one could here see the other wood polymers as a structure in parallel with the cellulose microfibrils. The results obtained here indicate that the straining of the structure on the molecular level, as detected by the FTIR signal, is the same with regard to the overall straining of the material, irrespective of whether the material is dry or moist. Under moist conditions, the accessible regions are softened and are then not able to carry much of the load, in comparison with the crystalline cellulose, i.e. if they were to take an active part in the loading, they would have to be deformed extensively. As this does not seem to be the case, this indicates that the moisture accessible regions must be located more on the cellulose microfibril surfaces than as regions along the length of the microfibrils. This fact is supported by the similarity in the behaviour for the pure cellulose sample. The accessible regions are probably not as extensive as to provide for a cooperative polymer molecular motion characteristic of a glass transition. However, their swelling as due to the moisture uptake would still imply a considerable reduction in its stiffness. Thus, the disturbed zones along the fibres must either be very small, inaccessible to the moisture in the RH region, or arranged in such a way that crystalline areas bridge most of these zones, consequently overcoming these weak zones. The potential existence of such a mixed structural distribution of the accessible regions needs though a more refined analysis. It is anyhow clear that the suggested structure supports the fact that the stiffness of the wood fibres is only marginally affected by moisture in the direction along the fibres (Kersavage 1973; Salmén 2004).

Summary

It has been demonstrated here that FTIR-spectroscopy may be used to monitor molecular straining during the loading of cellulosic materials. It was shown that the molecular deformation was linearly related to the macroscopic loading of the material. For wood alone, spectral deformations related to groups, assigned to the cellulose, were observed, while no molecular deformation could be detected for lignin or the hemicelluloses. Under moist conditions, the molecular straining of the cellulose molecule was greater with regard to the macroscopic force, when

compared to dry conditions, but equal with regard to the macroscopic strain. This could be interpreted in a way that moisture accessible regions are arranged more in parallel with the cellulose load bearing entities. Thus, it could be suggested that the cellulose disordered regions do not exist as large regions right across the cellulose aggregate structure, but that they are probably more spread out. In addition, the larger part of the moisture absorbing areas of the cellulose structure is probably related to the surface areas of the cellulose.

References

Agarwal UP (1999) An overview of Raman spectroscopy as applied to lignocellulosic materials. In: Argyropoulos DS (ed) Advances in lignocellulosics characterization. Atlanta, GA, TAPPI Press, USA, pp 209–225

Åkerholm M, Salmén L (2001) Interactions between wood polymers studied by dynamic FT-IR spectroscopy. Polymer 42(3):963–969. doi:10.1016/S0032-3861(00)00434-1

Åkerholm M, Salmén L (2003) The oriented structure of lignin and its viscoelastic properties studied by static and dynamic FT-IR. Holzforsch 57(5):459–465. doi:10.1515/HF.2003.069

Åkerholm M, Salmén L (2004) Softening of wood polymers induced by moisture studied by dynamic FT-IR spectroscopy. J Appl Polym Sci 94:2032–2040. doi:10.1002/app.21133

Bergander A, Salmén L (2002) Cell wall properties and their effects on the mechanical properties of fibers. J Mater Sci 37(1): 151–156. doi:10.1023/A:1013115925679

Burgert I, Gierlinger N, Eder M (2008) The mechanical properties of juvinile and adult wood tracheids—an insight into nanostructural deformation. In: Entwistle K, Harris P (eds) The compromised wood workshop 2007. J Walker Univ, Canterbury, pp 177–184

Cave ID (1968) The anisotropic elasticity of the plant cell wall. Wood Sci Technol 2:268–278. doi:10.1007/BF00350273

Colthup NB, Daly LH, Wiberley SE (1990) Introduction to infrared and raman spectroscopy. Academic Press, London

Eichhorn SJ, Sirichaisit J, Young R (2001) Deformation mechanisms in cellulose fibres, paper and wood. J Mater Sci 36(13):3129–3135. doi:10.1023/A:1017969916020

Fengel D (1991) Möglichkeiten und Grenzen der FTIR-Spektrokopie bei der Charakterisierung von CelluloseTeil 2. Vergleich von verschiedenen Zellstoffen Papier 45(3):97–102

Fengel D (1993) Influence of water on the OH valency range in deconvoluted FTIR spectra of cellulose. Holzforschung 47: 103–108

Gierlinger N, Schwanninger M, Reinecke A, Burgert I (2006) Molecular changes during tensile deformation of single wood fibers followed by Raman microscopy. Biomacromolecules 7(7):2077–2081. doi:10.1021/bm060236g

Hinterstoisser B, Åkerholm M, Salmén L (2001) Effect of fiber orientation in dynamic FTIR study on native cellulose. Carbohydr Res 334:27–37. doi:10.1016/S0008-6215(01)00167-7

Hinterstoisser B, Åkerholm M, Salmén L (2003) Load distribution in native cellulose. Biomacromolecules 4(5):1232–1237. doi:10.1021/bm030017k

Hofstetter K, Hinterstoisser B, Salmén L (2006) Moisture uptake in native cellulose—the roles of different hydrogen bonds: a dynamic FT-IR study using deuterium exchange. Cellulose 13(2):131–145. doi:10.1007/s10570-006-9055-2

Ivanova NV, Korolenko EA, Korolik EV, Zbankov RG (1989) Mathematical processing of IR-spectra of cellulose. Zurnal Prikladnoj Spektroskopii 51:301–306

Kersavage PC (1973) Moisture content effect on tensile properties of individual Douglas-Fir latewood tracheids. Wood Fiber 5(2):105–117

Liang CY, Marchessault RH (1959a) Infrared spectra of crystalline polysaccharides I. Hydrogen bonds in native celluloses. J Polym Sci 37:385–395. doi:10.1002/pol.1959.1203713209

Liang CY, Marchessault RH (1959b) Infrared spectra of crystalline polysaccharides. II. Native celluloses in the region from 640 to 1,700 cm^{-1}. Journal of Polymer Science 39:269–278. doi:10.1002/pol.1959.1203913521

Marechal Y, Chanzy H (2000) The hydrogen bond network in I.beta. cellulose as observed by infrared spectrometry. J Mol Struct 523:183–196. doi:10.1016/S0022-2860(99)00389-0

Page DH, El-Hosseiny F (1983) The mechanical properties of single wood pulp fibres Part VI, Fibril angle and the shape of the stress-strain curve. J Pulp Pap Sci Trans Techn Sect 9(4):99–100

Rowland SP, Roberts EJ (1972) The nature of accessible surfaces in the microstructure of cotton cellulose. J Polym Sci 10(Part A-1):2447–2461

Salmén L (1990) On the interaction between moisture and wood fiber materials. In: Caulfield DF, Passaretti JD, Sobczynski SF (eds) Materials Interactions Relevant to the pulp, paper, & wood ind, vol 197. Mater Res Soc, Pittsburgh, pp 193–201

Salmén L (2004) Micromechanical understanding of the cell-wall structure. C R Biol 327(9–10):873–880. doi:10.1016/j.crvi.2004.03.010

Sturcová A, Eichhorn SJ, Jarvis MC (2006) Vibrational spectroscopy of biopolymers under mechanical stress: processing cellulose spectra using bandshift difference integrals. Biomacromolecules 7:2688–2691. doi:10.1021/bm060457m

Tashiro K, Kobayashi M (1991) Theoretical evaluation of three-dimensional elastic constants of native and regenerated celluloses: role of hydrogen bonds. Polymer 32(8): 1516–1526. doi:10.1016/0032-3861(91)90435-L

Tsuboi M (1957) Infrared spectrum and crystal structure of cellulose. J Polym Sci 37:159–171. doi:10.1002/pol.1957.1202510904

Wickholm K, Larsson PT, Iversen T (1998) Assignment of non-crystalline forms in cellulose I by CP/MAS carbon 13 NMR spectroscopy. Carbohydr Res 312(3):123–129. doi:10.1016/S0008-6215(98)00236-5

Wool RP (1981) Measurements of infrared frequency shifts in stressed polymers. J Pol Sci 19(3):449–457